Ab Initio Modeling of Defect Signatures in Infrared Reflection−Absorption Spectra of SAMs Exposing Methyl- and Hydrogen-Terminated Oligo(ethylene glycols)

Lyuba Malysheva,[†] Alexander Onipko,[†] and Bo Liedberg*[,‡]

Bogolyubov Institute for Theoretical Physics, 03680 Kyiv, Ukraine, and Division of Molecular Physics, Department of Physics, Chemistry and Biology, Linköping University, S-581 83 Linköping, Sweden

Received: July 17, 2007; In Final Form: November 5, 2007

Extensive ab initio modeling has been performed to explain quantitatively the apparent shapes of characteristic bands, which are systematically observed in the fingerprint region of infrared (IR) reflection−absorption (RA) spectra of oligo(ethylene glycol) (OEG)-terminated SAMs. The *presence of defects* was thoroughly examined by modeling the RA spectra using the DFT method BP86/6-31G* for all-helical and all-trans conformers of $HS(CH_2CH_2O)_nR$ ($n = 5, 6$, $R = H, CH_3$) and $HS(CH_2)_{15}CONH(CH_2CH_2O)_6H$ molecules and for several defect-containing conformers. These data were then used to simulate RA spectra of SAMs with different content of defects and to compare them with experiments. It is shown that for SAMs of $HS(CH_2CH_2O)_nCH_3$ ($n = 5, 6$) the pronounced asymmetry of the dominating band can be attributed to the multimode nature of COC stretching vibrations of helical conformers combined with the contribution from few percent of all-trans conformers. Arguments are presented which disprove appreciable amounts of helical conformers with single trans and/or gauche defects. Much more complex combination of factors, which can come into play in the formation of the high-frequency shoulder of COC band, is exemplified by self-assemblies of OEG-terminated amide-bridged alkanethiolates. In particular, spectral signatures of defects with inverted OH terminus are compared with other contributions to the apparent shape of COC band formation. For this family of SAMs, the presence of about 10% of all-trans conformers gives a satisfactory quantitative agreement between the calculated RA spectra and experimental observations.

1. Introduction

Self-assembled monolayers (SAMs) generated from compounds with complex tail groups attract ever increasing research attention. In the field of new biomaterials, a substantial effort is focused on studies aiming at finding relationship between, on one hand, the conformational, wetting, and water adsorption characteristics of OEG segments and, on the other hand, the protein-repellent properties of OEG-containing SAMs. The OEG portion itself can be controlled and modified in a highly diverse manner. This possibility offers, in addition, a variety of applications in other fields of materials and surface science[1−6] as well as in molecular recognition and sensing[7] and molecular electronics.[8−11]

The sustained progress in these fields requires a deeper understanding of the geometry, precise positioning, and folding characteristics of the alkyl and OEG portions as well as the alkyl−OEG linkage group (if any) and the OEG-terminal head group. In the modeling of observed SAM infrared RA spectra, we have developed an improved understanding of the interrelation between the molecular structure (specifically, the head group and the conformational state of the OEG portion) and the shape of characteristic bands in SAM RA spectra.

As we have reported earlier,[12,13] comparison of IR RA spectra of two families of OEG containing SAMs with ab initio calculations unambiguously favors the helical OEG conformation as the most likely structure within these SAMs. In particular, it was shown that the fingerprint RA spectra monitored for self-assemblies of molecules $HS-EG_{5,6}CH_3$[14] and $HS-(CH_2)_{15}$-CONH-EG_6H[15] on gold (111) surfaces [here and later on, $EG_n \equiv (CH_2CH_2O)_n$], can be reproduced in all major features by the DFT method BP86/6-31G* applied for isolated molecular constituents. This is illustrated in Figure 1a,b, where the upper model spectra (i.e., middle curves in Figure 1a,b) were obtained as a sum of Lorentz peaks with the maxima proportional to the squared transition dipole moment (TDM) *z*-component of the respective vibration modes. The sum of the Lorentz peaks is taken over *nonscaled* frequencies, reproducing the frequencies of main peaks in the region within few cm^{-1}. Also, the intensity ratios of the dominating spectral features, the COC stretching and CH_2 wagging bands, agree very well with experimental observations.

The overall agreement between the first principle calculations and experiments points out the dominance of an *all-helical* conformation of the SAM OEG portion. However, the presence of other conformers, contributing to the band shape, cannot be refuted. Conformational defects can explain, at least partly, a number of minor divergences between theory and experiment. This has stimulated us to further study of subtle details of the SAM interior.

Two dominating bands of the SAM RA spectra are set in focus in this study. These are the band of COC stretching vibrations and the band of CH_2 wagging vibrations with maxima slightly below 1120 and 1350 cm^{-1}, respectively. The frequencies of these bands, as they were observed in experiments,[14,15] are summarized in Table 1 and compared with the results of our calculations.

* To whom correspondence should be addressed. E-mail: bolie@ifm.liu.se.
† Bogolyubov Institute for Theoretical Physics.
‡ Linköping University.

10.1021/jp075586r CCC: $40.75
Published on Web 01/08/2008

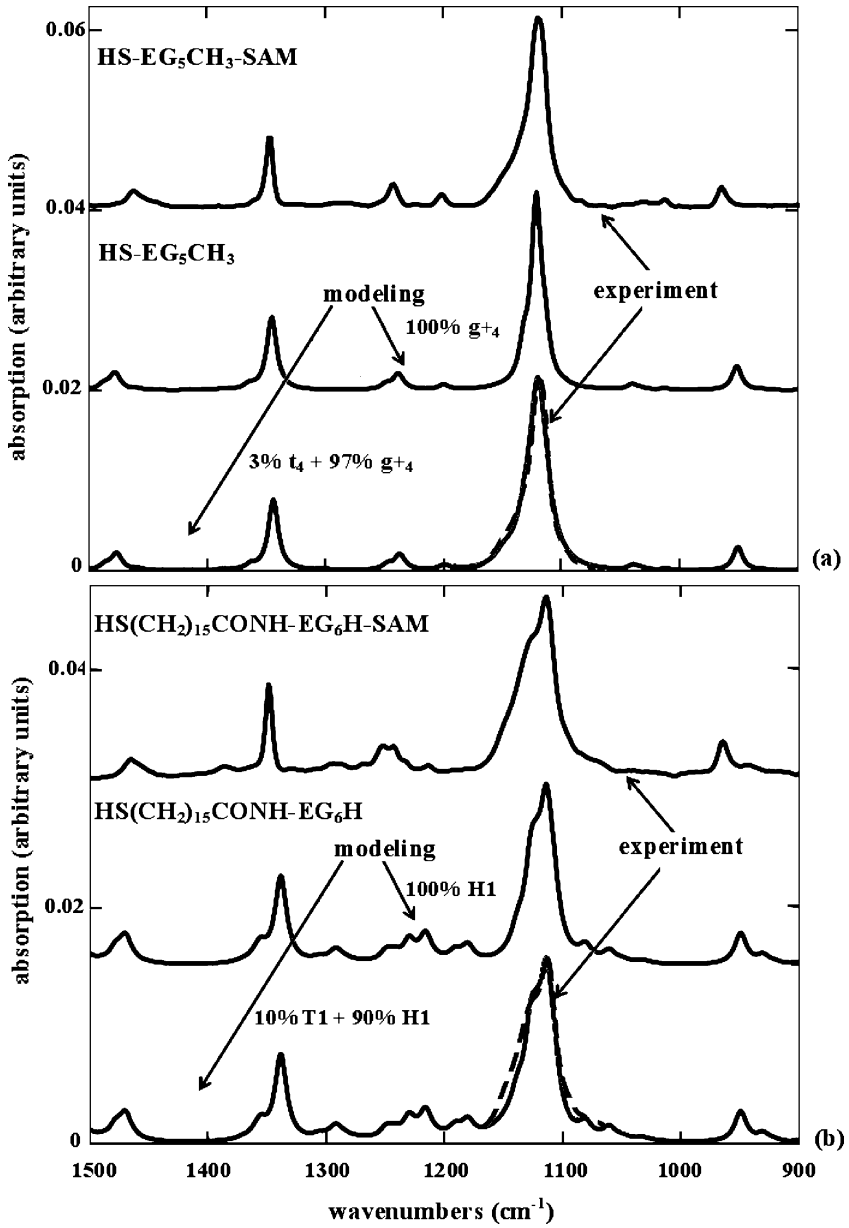

Figure 1. Experimental (upper curves, (a) HS−EG_5CH_3−SAM[14] and (b) $HS(CH_2)_{15}CONH-EG_6H$−SAM[15]) and calculated (middle and lower curves) RA spectra in the fingerprint region. Dashed curves on the model spectra repeat the COC band shape of observed experimental spectra. (a) Single molecule HS−EG_5CH_3 spectra correspond to the OEG helix axis perpendicular to the SAM surface: middle curve represents the spectrum of the all-helical conformer with hwhm (half-width at half-maximum) $\sigma = 5$ cm^{-1}, frequencies are not scaled; lower curve is the sum of the spectra of 97% all-helical and 3% all-trans conformers, where $\sigma = 8$ cm^{-1} for the main peak and $\sigma = 5$ cm^{-1} for the rest of the spectrum (for all frequencies, scaling factor is equal to 1.006). (b) Single molecule $HS(CH_2)_{15}CONH-EG_6H$ spectra correspond to $\theta_A = 26°$, $\psi_A = -62°$, as found in ref 13. The definition of Euler angles θ_A (*z*-axis tilt) and ψ_A (CCC-plane rotation) is borrowed from Parikh and Allara.[16] Orientation of OEG chain with respect to the substrate surface is defined similarly by tilt and rotation angles θ_E and ψ_E; see also ref 13. Middle curve represents the spectrum of the all-helical conformer with hwhm $\sigma = 6$ cm^{-1}, frequencies are not scaled; lower curve is obtained as the sum of the spectra of 90% all-helical conformers with $\sigma = 6$ cm^{-1} and 10% all-trans conformers with $\sigma = 20$ cm^{-1}. The frequency scaling factor equals 1.002. Notations g^+_n, t_n, H1, and T1 are explained in the text.

The asymmetry of the COC band, which is clearly seen in the RA spectra, has been observed in many studies of highly ordered OEG-containing SAMs. Our previous modeling, represented by the middle curves in Figure 1a,b, reproduces to some extent the appearance of a high-frequency wing and shoulder in the RA spectra of methyl- and hydrogen-terminated SAMs. However, neither the wing nor the shoulder calculated for the all-helical conformers agrees particularly well with that we see in the experimental RA spectra.

It is known that the equilibrium energies for many of the investigated OEG conformers (including the all-trans) do not differ much from each other.[17] In a recent study,[18] however, we have found a specific helical conformational state of hydrogen-terminated OEG-SAM, which has a substantially lower energy in comparison with the all-helical and all-trans conformers. Another distinctive feature of the new conformation is that the terminal OCCO dihedral angles are quite far from the typical "helical value".

In this work, we have admitted the presence in SAMs of several intramolecular defects and examined the RA spectra of defected helical and all-trans conformers of molecules $HS(CH_2-CH_2O)_nR$ ($n = 5$, 6, R = H, CH_3) and $HS(CH_2)_{15}CONH(CH_2-CH_2O)_6H$. As an outcome, an improved quantitative description

TABLE 1: Comparison of the Observed Spectral Position of Band Maximum and Shoulder with the Calculated Frequencies of the Most Intense and Next-Intense Modes of COC Stretching and CH_2 Wagging Vibrations for Several Molecules Containing OEG Portion in All-Helical Conformation

	asym COC stretching vibrations freq (cm^{-1}) peak max		asym COC stretching vibrations freq (cm^{-1}) shoulder		CH_2 wagging vibrations freq (cm^{-1}) peak max	
type of vibrations/ molecule and SAM	observed	calculated	observed	calculated	observed	calculated
$HS-EG_5CH_3$[14]	1118	1113	N/O[a]		1347	1336
$HS-EG_6CH_3$[14]	1118	1110	N/O		1347	1335
$HS-EG_5H$	N/A[a]	1112	N/A	1127	N/A	1337
$HS-EG_6H$	N/A	1110	N/A	1124	N/A	1335
$HS(CH_2)_{15}CONH-EG_6H$[15]	1114	1111	1127	1125	1349	1336

[a] N/A and N/O stand for respectively "not available" and "not observed".

of the observed RA spectra has been obtained which is illustrated by lower curves in Figure 1a,b.

2. Low-Energy Conformers of Methyl- and Hydrogen-Terminated Oligo(ethylene glycols)

The equilibrium conformer geometries of 1-thio(oligo)-ethylene glycols SH-EG_nR, where R = CH_3 and H and n = 5, 6, were calculated by using BP86 DFT method with 6-31G* basis set as provided by Gaussian-03. In a series of previous studies of IR RA spectra of these and related SAMs,[12,13,19] this method has been identified as an optimal one in terms of reliability and computational time. In particular, it gives practically the same results as those obtained by Wang et al.[17] for similar but shorter OEG strands $CH_3-EG_n-CH_3$ (n = 3, 4) with a larger basis BP86/6-311++G**. In notations of the quoted work, all-helical conformation of EG_n reads as g^+_{n-1} (= $g^+g^+g^+g^+$ for n = 5), where $g^{+(-)}$ = ($tg^{+(-)}t$) denotes *gauche* clockwise (anticlockwise) conformers of the OCCO unit with positive (negative) dihedral angle τ(OCCO). In analogy with g-notations, all-trans EG_n conformer is denoted as t_{n-1}, t = (ttt). Table 2 relates structural details of studied conformers with their symbolic indication.

The all-helical and all-trans conformers, and the conformers with one trans defect at either end of the OEG helical chain, $g^+_{n-2}t$ and tg^+_{n-2}, possess an energy difference of the order of 0.3 kcal/mol or less. This is true for both methyl- and hydrogen-terminated 1-thio-OEGs (see Table 3). Similar results are expected to be valid for longer molecules, where EG_n conformers are covalently bound with an alkyl chain. In support of this conclusion, comparison of all-helical (H1) and all-trans (T1) conformers of molecule $HS(CH_2)_{15}CONH-EG_6H$ shows that the difference between conformational energies of H1 and T1 (also given in Table 3) is of the same order and sign as that is found for the respective conformers of $HS-EG_6H$.

In the case of methyl-terminated OEGs, we concentrate our discussion on defects t_{n-1}, $g^+_{n-2}t$, and tg^+_{n-2} in SAMs of g^+_{n-1} conformers. Several other conformers with close energies, which initially were considered as possible defects, give RA spectra that are inconsistent with experimental observations. Therefore, they were eliminated from the list of potential defects. For example, conformers of the type $g^+g^+g^-g^+$ (shown in the second line from below in Table 2) have received much attention as potential "water binders".[17] However, they are disregarded here as likely defects in well-ordered SAM structures on the grounds of steric constraints and a large disagreement between the calculated and observed shape of the COC stretching and CH_2 wagging bands (see the Supporting Information).

In the case of a hydrogen-terminated OEGs, a new conformer should be taken into account which, unlike the all-helical conformation, has a *pointing-down* orientation of the O−H bond[18] (see Figure 2). This equilibrium geometry, denoted in Table 3 as $g^+_{n-2}\bar{g}$, has a much lower energy than g^+_{n-1}. It can be thought as a result of a distortion of gauche terminal dihedral angle, τ(OCCO) → τ^L(OCCO), accompanied by a considerable reorientation of the terminal O−H group. In the $g^+_{n-2}\bar{g}$ configuration, the O−H bond is nearly inverted as compared to its orientation in the g^+_{n-1} configuration. A similar conformer of the $HS-(CH_2)_{15}CONH-EG_6H$ molecule with inverted O−H bond, H2, displays nearly as large an energy drop in comparison with H1. This indicates that the energy gain due to the transformation H1 → H2 is almost completely determined by the inversion of O−H bond. It is noteworthy that the inversion of the O−H bond in all-trans conformers of the $HS-(CH_2)_{15}$-$CONH-EG_6H$ molecule (all-trans equilibrium geometries of the composed molecules with upward and downward orientation of O−H bond are denoted as T1 and T2, respectively) has a much smaller effect on the conformational energy (see Table 3). Again, calculations performed for all trans OEGs with and without an alkyl tail give nearly the same energy difference between conformers with O−H bond pointing up and down.

The substantially lower energies of $g^+_{n-2}\bar{g}$ and H2 conformations are due to a greatly reduced distance between the O−H hydrogen and the next-nearest oxygen (see Figure 2). In view of the large energy gain, one can assume that the constituent molecules of the $HS-(CH_2)_{15}CONH-EG_6$ SAMs adopt the H2 conformation. This is supported by first principle calculations of the equilibrium geometry of periodical arrays of molecules analogues but shorter than those encountered herein.[18] In what follows, we examine the consistency of this particular assumption, as well as the possibility of presence of other conformers, which differ from all-helical, by comparing the model spectra with the experimentally observed RA spectra represented in Figure 1.

3. Effects of End Group and OEG Conformation on the Shape of Characteristic Bands

The close energies of the conformers discussed in the preceding section and the steric semblance of their geometries can be used as arguments in favor of presence of defected (i.e., not ideally helical) conformers in self-assemblies of $HS-EG_n-CH_3$ and $HS-(CH_2)_nCONH-EG_mH$. In its turn, this might be the reason for the divergence between the observed band shape of the dominant band of COC stretching vibrations and its reproduction on the basis of an all-helical, defect-free, model of the OEG portion. We have studied the soundness of these assumptions by modeling RA spectra of conformers g^+_{n-1}, $g^+_{n-2}t$, tg^+_{n-2}, t_{n-1}, $g^+_{n-2}\bar{g}$, H1(2), and T1(2). With this purpose in mind, the TDMs of the vibration modes were calculated with the same precision as was employed to obtain the optimized

TABLE 2: All-Helical, Helical with One and Two Trans Defects, Helical with Single Gauche Defect, and All-Trans Conformations of the HS−EG$_5$CH$_3$ Molecule and Their Symbolic Representation Borrowed from Ref 17

Notation	Schematic representation	Drawing
g^+_4 = $g^+g^+g^+g^+$	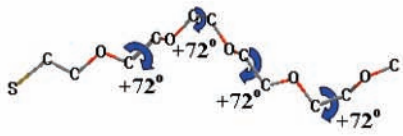	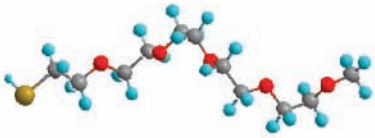
g^+_3t = $g^+g^+g^+t$	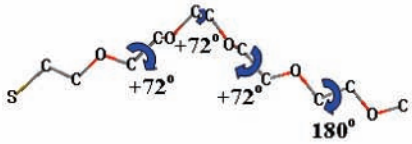	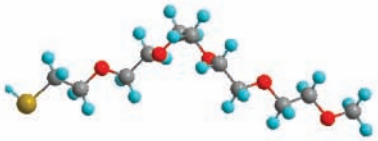
tg^+_3 = $tg^+g^+g^+$	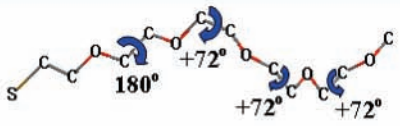	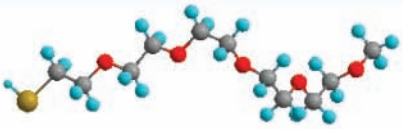
$g^+_2t_2 = g^+g^+tt$	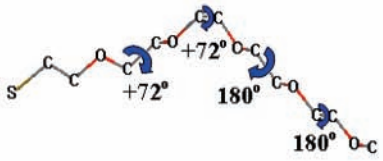	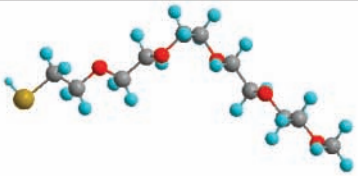
$g^+g^+g^-g^+$	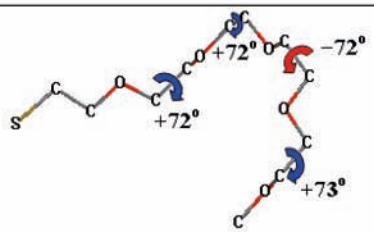	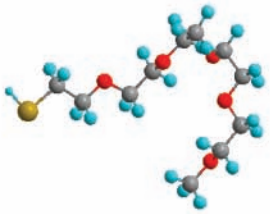
$t_4 = tttt$	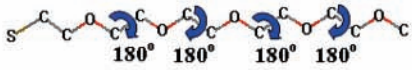	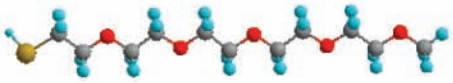

TABLE 3: Relative Energies of Conformers of Molecules HS−EG$_n$R (n = 5,6, R = CH$_3$, H) and HS−(CH$_2$)$_{15}$CONH−EG$_6$H

molecule/conformer[a]	HS−EG$_5$−CH$_3$ energy, kcal/mol	HS−EG$_6$−CH$_3$	HS−EG$_5$−H	HS−EG$_6$−H	HS−(CH$_2$)$_{15}$CONH−EG$_6$H energy, kcal/mol	
g^+_{n-1}	0	0	0	0	H1	0
$g^+_{n-2}t$	−0.07	−0.06	−0.27	−0.33		
tg^+_{n-2}	0.02	0.03	0.03	0.02		
t_{n-1}	0.05	0.08	−0.17	−0.16	T1 (T2)	−0.09 (−0.67)
$g^+_{n-2}\bar{g}$			−4.16	−3.93	H2	−3.99

[a] For shorter molecules, g^+ = (tg^+t) denotes *gauche* clockwise conformer of the OCCO unit. For the longer molecule, all-helical and all-trans conformers are denoted as H1 and T1, respectively; their counterparts with an inverted O−H bond are H2 and T2. SCCO unit is in the trans conformation. For helical conformers, all dihedral angles τ(OCCO) are about ∼70°, except the terminal dihedral in $g^+_{n-2}\bar{g}$ and H2 conformations, where τ^L(OCCO) = 59°. In molecules g^+_{n-1}, H1, and T1, τ(CCOH) = −170°, −170°, and 179°, respectively; in molecules $g^+_{n-2}\bar{g}$, H2, and T2, τ(CCOH) = −49°, −49°, and −68°, respectively.

configurations. Then, the model RA spectra in the fingerprint region were simulated according the procedure described in ref 12.

3.1. Choice of Molecule Orientation. To our knowledge, the molecule orientation in SAMs of HS−EG$_n$CH$_3$ was never addressed quantitatively. Most often, the molecular axis is assumed to be perpendicular to the SAM surface. This is in good agreement with experiment (see Figure 1a). Therefore, RA spectra of HS−EG$_n$CH$_3$ conformers were calculated with the tilt angle of the OEG axis θ_E set to zero. In this connection, it should be stressed that in the fingerprint region, the shape of the RA spectrum of conformer g^+_{n-1} remains essentially unchanged under rather large variation of the molecule orientation $0 < \theta_E < 30°$ because the z-component of the TDMs is

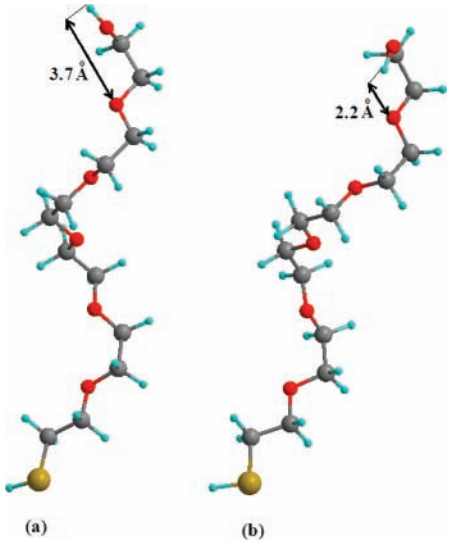

Figure 2. BP86/6-31G* optimized geometries of HS−EG_6H molecule in helical conformation with (a) *pointing-up* (g^+_5) and (b) *pointing-down* ($g^+_4\bar{g}$) orientation of the O−H bond.

dominating for all characteristic vibrations in the fingerprint region. As a consequence, the appearance of the model RA spectra is weakly dependent on θ_E. An analysis of CH_2 stretching region[12] is more in favor of nonzero tilt of OEG-axis, but the precise molecular orientation within SAMs of 1-thio-oligo(ethylene glycols) is still open to question.

For SAMs consisting of composed molecules (alkyl-amide-OEG), zero tilt angle θ_E contradicts the observed spectrum in the CH_2 stretching region. The molecule orientation in SAMs of H1 conformers of HS−$(CH_2)_{15}$CONH-EG_6H, $\theta_A = 26°$, $\psi_A = -62°$ ($\theta_E = 22°$, $\psi_E = 25°$), was deduced from a comparison of experimental and model RA spectra.[13] [Orientation of OEG chain with respect to the substrate surface is defined similarly to the orientation of alkyl chain, i.e., by Euler tilt and rotation angles θ_E and ψ_E; see for details ref 13.] Here, the same orientation is assumed to be valid for the evaluation of the contribution into the apparent RA spectra from conformers H2, T1, and T2.

3.2. Band of COC Stretching Vibrations. We begin with an analysis of vibration modes. Specifically, in focus is the dependence of the mode intensity distribution on the end groups and oligomer length. Figure 3 shows relative mode intensities within the COC band calculated for all-helical conformation of HS-EG_nR (R = CH_3, H, n = 5, 6).

For HS−$EG_{5(6)}CH_3$ molecules in all helical conformation g^+_4 (g^+_5), the main peak near 1113 cm^{-1} agrees very well with that is recorded experimentally.[14] The replacement of the methyl end group by hydrogen has a marginal effect on the spectral position of the peak maximum (see Table 1) but results in a substantial redistribution of the mode intensities. In agreement with the experiment, the presence of a high-frequency shoulder of COC band is clearly associated with an OH terminus. In presence of the latter, there exists an intense mode of COC skeleton vibrations (at 1124 cm^{-1}) that involves motion of the O−H bond. Thus, the 1124 cm^{-1} mode is most likely an inherent feature of hydrogen-terminated OEGs, which does not appear in the spectrum of SAMs consisting of methyl-terminated OEGs. According to these calculations, the high-frequency shoulder on the band of COC stretching vibrations should only be present for hydrogen-terminated OEG chains. Also for conformers with a trans defect near the terminus, the mode intensity distribution is very sensitive to whether the terminus is a methyl or hydrogen (see Figure 3). We return to this point later on.

In interests of clarity, we proceed with a separate discussion of relevance of the model conformer spectra to experiments for

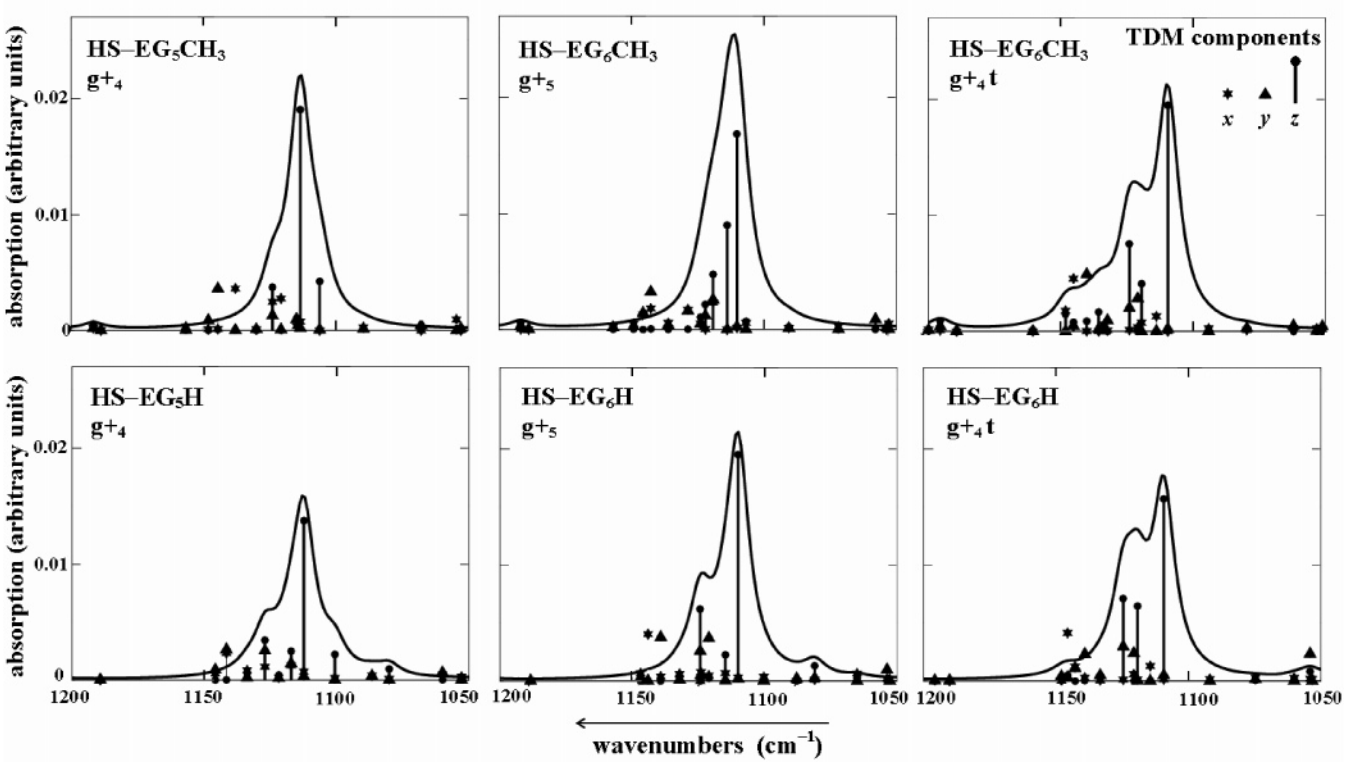

Figure 3. Band of COC stretching vibrations calculated for g^+_{n-1} and g^+_4t conformers of HS−EG_nCH_3 (top panel) and HS−EG_nH (bottom panel); n = 5, 6. Stars, triangles, and filled circles with vertical bars indicate relative magnitude of *x*-, *y*-, and *z*-TDM components, respectively; hwhm = 5 cm^{-1}. OEG axis is perpendicular to the SAM surface.

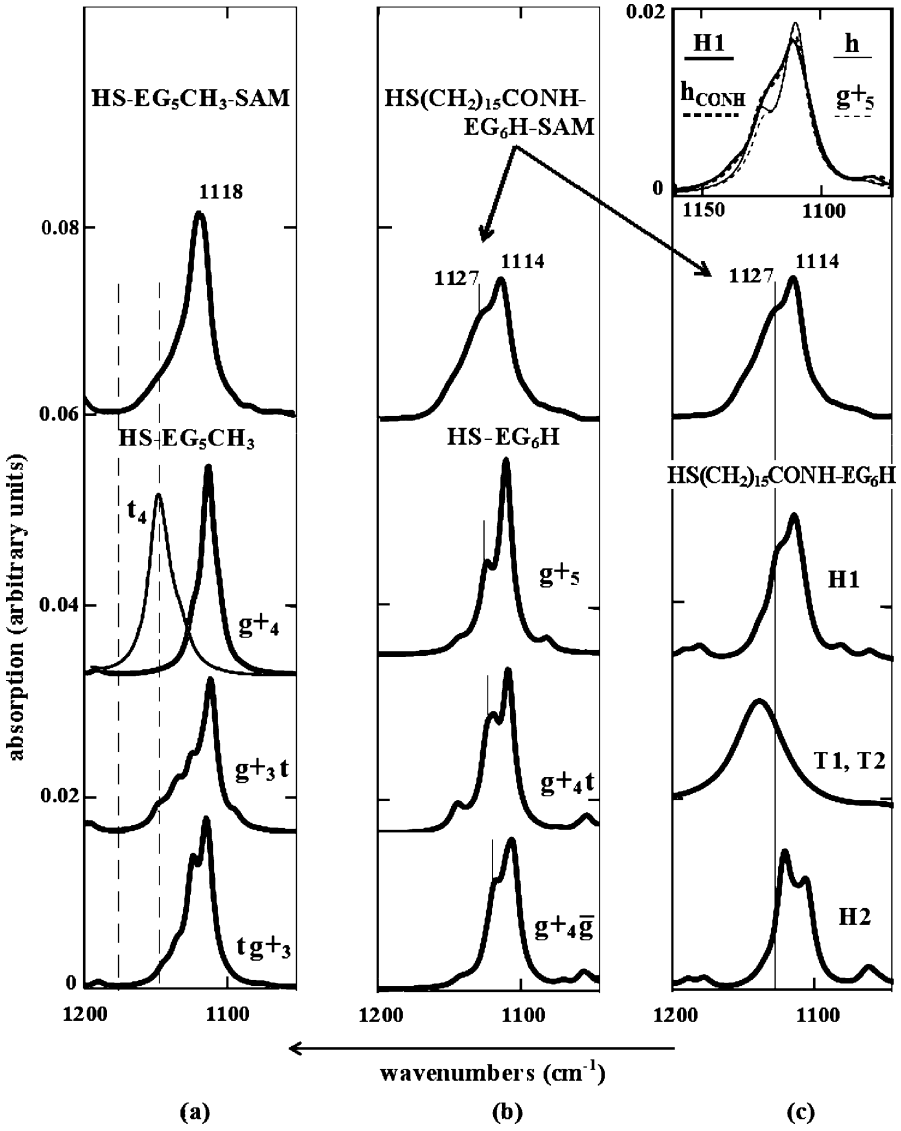

Figure 4. Upper curves show the COC band shape as it is observed in SAMs of HS−EG_5CH_3[14] (first column) and HS−$(CH_2)_{15}$CONH−EG_6H[15] (second and third column). Other curves: (a) COC band shape calculated for the conformers g^+_4, t_4, g^+_3t, and tg^+_3 of molecule HS-EG_5CH_3; (b) g^+_5, g^+_4t, and $g^+_4\bar{g}$ of molecule HS-EG_6H; and (c) H1, H2, T1, and T2 of molecule HS−$(CH_2)_{15}$CONH−EG_6H. The hwhm was set 5 cm^{-1} for all molecules HS−$EG_{5,6}R$ (except conformation t_4, for which hwhm = 8 cm^{-1}); hwhm = 6 cm^{-1} for conformers H1, H2, and 20 cm^{-1} for conformers T1, T2. Upper inset in the third column: COC band calculated for the all-helical conformation of molecules H1 (thick-solid lines), $HS(CH_2)_3$-CONH−EG_6H = h_{CONH} (thick-dashed lines), $HS(CH_2)_5$−EG_6H = h (thin-solid lines), and HS−EG_6H (thin-dashed lines). In calculations represented in the inset, the OEG axis is perpendicular to the SAM surface and hwhm = 6 cm^{-1}.

CH_3- and H-terminated SAMs. COC bands of the conformer g^+_4 with CH_3 terminal and g^+_5 with H terminal are shown again in Figure 4, where they can be directly compared with the appearance of this band in experimental RA spectra of SAMs of HS−EG_5−CH_3[14] and HS−$(CH_2)_{15}$CONH−EG_6H[15] and in the model spectra for other conformers listed in Table 3.

3.2.1. Methyl-Terminated SAMs. As already mentioned, the all-helical conformer does not have optically active vibration modes which could explain the apparent wing, which extends well above the shoulder at 1124 cm^{-1}; in Figure 4a, it is marked by two vertical dashed lines. It is also seen that neither of conformers $g^+_{n-2}t$ or tg^+_{n-2} with single trans defects has sufficiently active modes in the wing frequency region, suggesting that a single all-trans defect either at the terminus or close to the SH group cannot explain the presence of a high-frequency wing. Moreover, in the subsequent mode analysis of the band of CH_2-wagging vibrations (see section 3.3), we present another strong argument objecting the presence of a noticeable amount of single trans defects in SAMs of HS−EG_n−CH_3, n = 5, 6. It seems natural to admit that a larger hwhm would eliminate the divergence between the calculated and observed COC band shape, but it does not. Instead, our modeling shows that a certain amount of t_4 (all-trans) guest conformers in SAMs of g^+_4 HS−EG_5−CH_3 host conformers markedly improves the agreement between theory and experiment. For example, the spectrum calculated for the 97% all-helical and 3% all-trans conformers makes the COC band shape almost indistinguishable from that is observed experimentally (see the lower curve in Figure 1a).

3.2.2. Hydrogen-Terminated SAMs. Figure 4b reveals the shape of COC band obtained for g^+_5, g^+_4t, and $g^+_4\bar{g}$ conformers of HS-EG_6H. Because experimental data on self-assemblies of hydrogen-terminated 1-thio(oligo)ethylene glycols are not available, we compare our calculations with RA spectra of SAMs which additionally contains alkyl and amide parts.[15] The spectral appearance of COC band for H1 (related to g^+_5) and H2 (related to $g^+_4\bar{g}$) conformers, and for all-trans conformers of HS−$(CH_2)_{15}$CONH-EG_6H with upward (T1) and downward (T2)

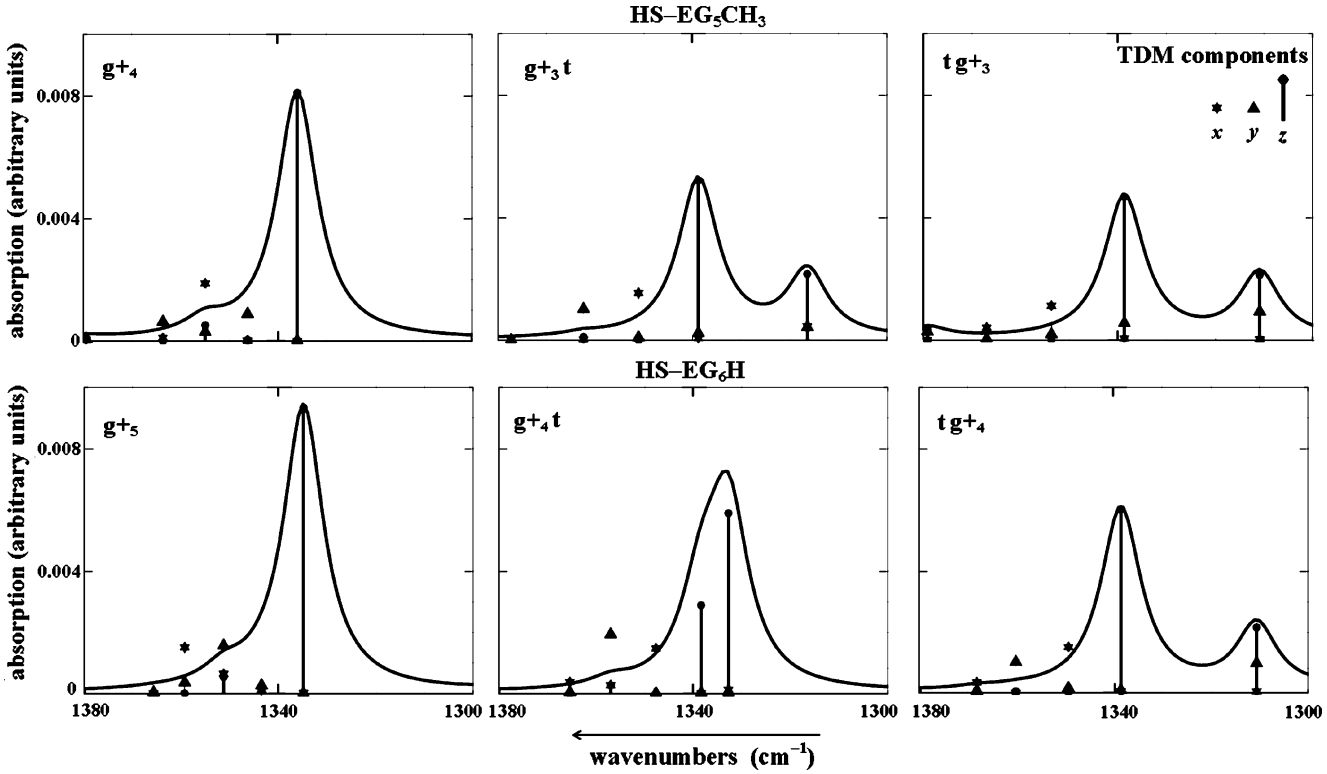

Figure 5. RA spectrum in the region of CH_2 wagging vibrations calculated for all-helical and defected helical conformers of HS−EG_5CH_3 (top panel) and HS−EG_6H (bottom panel). Molecular orientation, hwhm, and indication of TDM components are the same as in Figure 3.

directed O−H bond, is shown in Figure 4c. As immediately follows from this comparison, the alkyl−amide part of the molecule has a profound effect on the band shape. The effect is manifested by strengthening of the intensity of the high-frequency shoulder. It is so strong that the apparent shape of COC band changes. Indeed, for HS−EG_6H molecule in the conformation g^+_5, the second intense mode reveals itself as a nearly resolved maximum about half as strong as the main peak. But in the amide-containing H1 molecule, this feature converts into a vaguely resolved shoulder with an intensity nearly equal to that of the main peak. In conformers with inverted O−H bond, the effect of OEG−alkyl connection via amide bridge is even stronger: the shoulder in the spectrum of $g^+_4\bar{g}$ converts into the main peak of the H2 spectrum. The aforementioned spectral changes cannot be attributed to the tilt of OEG axis in molecules H1 and H2 because, first, the tilt angle θ_E is not large enough and, second, the intensities of both modes should be affected almost equally as they are z-modes.

To further clarify the origin of the shoulder on the COC-band observed at ∼1125 cm^{-1} in self-assemblies of HS−$(CH_2)_{15}$CONH-EG_6H,[15] we have performed additional calculations for molecules containing the alkyl and OEG parts but without amide linkage group, that is, HS$(CH_2)_5$-EG_6H = h and HS$(CH_2)_3$CONH-EG_6H = h_{CONH}, both with a much shorter alkyl chain. For the all-helical conformation of these molecules, the band of COC-stretching vibrations is represented in the inset together with g^+_5 and H1 bands. In all four molecules, the EG_6H tail is the same and equally oriented, and we used the same hwhm in the spectral modeling. As follows from these calculations, the presence or absence of the alkyl tail and its length produce minor effects on the COC band shape. In contrast, the amide linkage group has a clear signature that manifests itself in a noticeable enhancement of the high-frequency component of COC band.

Additional evidence in support of that the redistribution of intensities between two most intense modes of COC stretching vibrations of hydrogen-terminated OEGs is caused by amide group can be found in spectra of several related SAMs. For example, in SAMs without amide bridge, such as SAMs of HS-$(CH_2)_9$−EG_7H, the high-frequency shoulder observed at ∼1125 cm^{-1} in ref 15 and at ∼1130 cm^{-1} in ref 20 has a lower relative intensity with respect to the main peak than in SAMs of amide-bridged, OEG-terminated alkanethiolates such as HS$(CH_2)_{11}$-CONH−EG_6H.[15]

As follows from this modeling, of two possible geometries with upward and downward orientation of O−H bond, H1 and H2, only H1 reasonably reproduces the observed COC band at 1114 cm^{-1}. To recall, the H2 conformer has ∼4 kcal/mol lower energy than the H1 conformer. In the calculated spectrum of the latter, the high-frequency wing of the dominating COC band is not reproduced sufficiently well. Guided by the same arguments as in the modeling performed for SAMs of HS−$EG_{5,6}CH_3$, we have admitted a contribution originating from all-trans conformers to the apparent COC band shape. The best fit is attained with about 10% of defects T1 (or T2, or both) and a somewhat larger broadening of the defect component in the corresponding RA spectrum. The spectrum simulating a SAM with 90% of host molecules H1 and 10% of defects T1 is represented by the lower curve in Figure 1b, where dashed line indicates the shape of the observed COC band.

Thus, the comparison of model and experimental spectra represented in Figure 4 rejects the lowest energy conformer H2 with inverted O−H bond, as the host molecules in respective SAMs. Unfortunately, the lack of experimental data does not allow us to evaluate the role of these conformers in more detail. For this, as well as for the other open issues of formation OEG-containing SAMs, it would be highly informative to have RA spectra of SAMs of HS-EG_nH.

3.3. Band of CH_2 Wagging Vibrations. Results of our calculations of TDMs of the CH_2 wagging vibration modes are represented in Figure 5. For all-helical conformers, g^+_4 and g^+_5, the band shape is essentially the same for the two end groups,

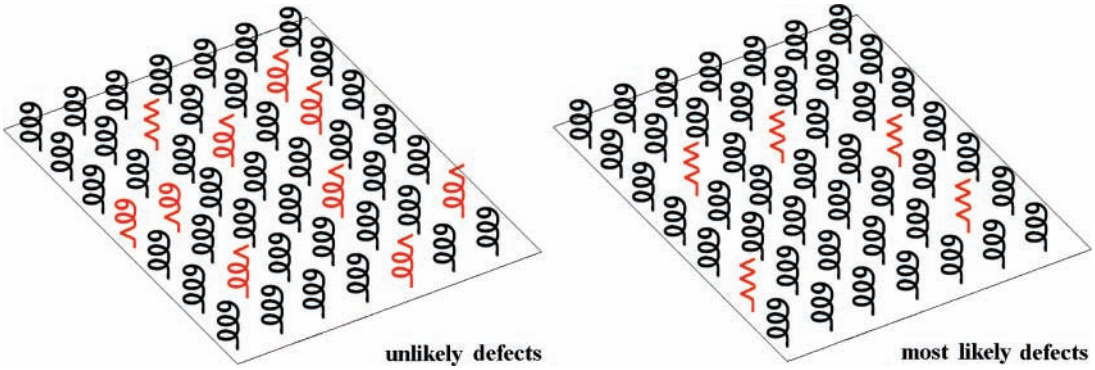

Figure 6. Cartoon describing the unlikely and likely distribution of defects in an OEG-terminated SAMs as it follows from the modeling. Black: all-helical OEGs; red: OEGs with one trans unit and all-trans OEGs.

methyl and hydrogen. This is in agreement with experiment, where for CH_3- and H-terminated SAMs the bands at 1347 and 1349 cm^{-1} have very similar appearance (see Figure 1). In contrast, for helical conformers with single trans defects, the shape of wagging band differs much depending on which group terminates OEG chain. Methyl-terminated conformers have two instead of one intense vibration mode. An additional (lower frequency) intense mode involves collective vibrations of CH_2 groups which belong to the trans OCCO unit and its nearest neighbor. In the experimental spectra, no traces of the wagging band splitting can be found, thus objecting the presence of helical conformers with single trans defects—at least in the amount that is sufficient for detection by means of IR RA spectroscopy.

4. Conclusion

The focus of this study has been on the so-called fingerprint region of IR spectrum, where OEG vibration modes dominate the response. Therefore, all significant features in this part of the spectrum were interpreted (explicitly or silently) as a contribution coming exclusively from vibrations of ethylene glycol chains. However, this modeling show that in SAMs containing an amide bridge group the high-frequency shoulder of COC band cannot be assigned exclusively to COC stretching vibrations. For the family of self-assemblies of OEG-terminated, amide-bridged alkanethiolates, the shoulder should be understood as a signature of coupled amide−OEG vibrations. This coupling strongly enhances the COC band shoulder, which is shown to be characteristic for hydrogen-terminated, but not for methyl-terminated, OEGs. Furthermore, the shoulder should be understood as a manifestation of multimode character of COC stretching vibrations and not as a spectral appearance of defects, often stated in previous studies.[15,20,21]

Ab initio modeling of the observed shape of the bands of COC stretching and CH_2 wagging vibrations rules out the presence of helical conformers with single trans defects in SAM OEG moiety—at least in the amount affecting apparent IR RA spectra. In contrast, the presence of a substantial amount of defects in the form of all-trans conformers (see Figure 6) is shown to be very likely, giving a much better agreement between theory and experiment. In the case of self-assemblies of SH-$EG_{5,6}CH_3$, 3% of these defects fit almost perfectly the observed shape of COC band. The same modeling suggests that in SAMs of EG_6H-terminated amide-bridged alkanethiolates the content of trans defects is higher, most likely about 10%. However, for SAMs generated from such large and complex constituents, the obtained agreement with experiment is somewhat less convincing. This is attributed to the limited accuracy of these very demanding calculations.

The above conclusions and those singled out throughout preceding discussion are based on rather accurate but not exact calculations. Therefore, many of important points were cross-checked with the help of more accurate but still approximate methods. In this connection, comparison with a larger wealth of high-resolution spectroscopy data is required. In particular, comparison of mode intensity distributions represented in Figure 3 with spectra of self-assemblies of $SH-EG_{5,6}H$ would provide us with, on one hand, an additional check of accuracy of this description and, on the other hand, an additional source of information about subtle effects of intramolecular interactions. This is a challenging task for the future. Single-molecule approximation is another inherent weakness of this and all other ab initio based studies in the field. Only recently, first preliminary results on full account of intermolecular interactions in 2D periodical arrays have been reported.[18] Further work in this direction is in progress.

Acknowledgment. This work was supported by the Swedish Foundation for Strategic Research (SSF), the Visby program (SI), the Swedish Research Council (VR), and the Royal Academy of Science (KVA). We also express our gratitude to Prof. David Vanderah for supplying us with infrared data of the methoxy-terminated SAMs.

Supporting Information Available: Figure SI showing the measured spectrum of $HS-EG_5CH_3-SAM$[14] and modeled spectra of several conformations of methyl-terminated OEGs in the fingerprint region; Figures SII and SIII showing the measured spectrum of $HS(CH_2)_{15}CONH-EG_6H-SAM$[15] and calculated spectra of several conformations of hydrogen-terminated OEGs in the same frequency interval. This information is available free of charge via the Internet at http://pubs.acs.org.

References and Notes

(1) Nuzzo, R. G.; Allara, D. L. *J. Am. Chem. Soc.* **1983**, *105*, 4481.
(2) Laibinis, P. E.; Hickman, J. J.; Wrighton, M. S.; Whitesides, G. M. *Science* **1989**, *245*, 845.
(3) Prime, K. L.; Whitesides, G. M. *Science* **1991**, *252*, 1164.
(4) Laibinis, P. E.; Whitesides, G. M.; Allara, D. L.; Tao, Y.-T.; Parikh, A. N.; Nuzzo, R. G. *J. Am. Chem. Soc.* **1991**, *113*, 7152.
(5) Ulman, A. *Chem. Rev.* **1996**, *96*, 1533.
(6) Schreiber, F. *Prog. Surf. Sci.* **2000**, *65*, 151.
(7) Lahiri, J.; Isaacs, L.; Tien, J.; Whitesides, G. M. *Anal. Chem.* **1999**, *71*, 777.
(8) Tour, J. M.; Jones, L.; II; Pearson, D. L.; Lamba, J. S.; Burgin, T.; Whitesides, G. M.; Allara, D. L.; Parikh, A. N.; Atre, S. *J. Am. Chem. Soc.* **1995**, *117*, 9529.
(9) Reed, M. A.; Zhou, C.; Muller, C. J.; Burgin, T. P.; Tour, J. M. *Science* **1997**, *278*, 252.

(10) Chen, J.; Reed, M. A.; Rawlett, A. M.; Tour, J. M. *Science* **1999**, *286*, 1550.
(11) Wold, D. J.; Frisbie, C. D. *J. Am. Chem. Soc.* **2001**, *123*, 5549.
(12) Malysheva, L.; Onipko, A.; Valiokas, R.; Liedberg, B. *J. Phys. Chem. B* **2005**, *109*, 13221.
(13) Malysheva, L.; Onipko, A.; Valiokas, R.; Liedberg, B. *J. Phys. Chem. A* **2005**, *109*, 7788.
(14) Vanderah, D. J.; Arsenault, J.; La, H.; Gates, R. S.; Silin, V.; Meuse, C. W. *Langmuir* **2003**, *19*, 3752.
(15) Valiokas, R.; Östblom, M.; Svedhem, S.; Svensson, S. C. T.; Liedberg, B. *J. Phys. Chem. B* **2001**, *105*, 5459.
(16) Parikh, A. N.; Allara, D. L. *J. Chem. Phys.* **1992**, *96*, 927.
(17) Wang, R. L. C.; Kreuzer, H. J.; Grunze, M. *Phys. Chem. Chem. Phys.* **2000**, *2*, 3613.
(18) Malysheva, L.; Onipko, A.; Liedberg, B. *Phys. Status Solidi B* **2006**, *243*, 3489.
(19) Malysheva, L.; Onipko, A.; Valiokas, R.; Liedberg, B. *Appl. Surf. Sci.* **2005**, *246*, 372.
(20) Harder, P.; Grunze, M.; Dahint, R.; Whitesides, G. M.; Laibinis, P. E. *J. Phys. Chem.* **1998**, *102*, 426.
(21) Vanderah, D. J.; Valincius, G.; Meuse, C. W. *Langmuir* **2002**, *18*, 4674.